Rev. Adv. Mater. Sci. 45 (2016) 20-27

MICROSTRUCTURE TRANSFORMATION IN A CAST Cu-Fe ALLOY AT HIGH PRESSURE TORSION DEFORMATION

A. Lukyanov[1], A. Churakova[2], D. Gunderov[2,3], A. Filatov[4], E. Antipov[4], V. Sitdikov[2,5], A. Ganeev[2], R. Valiev[2,5] and V. Pushin[1]

[1]Ural Division of Russian Academy of Sciences, Institute of Metal Physics, 18 S. Kovalevskaya str., Ekaterinburg 620041, Russia
[2]Ufa State Aviation Technical University, K. Marx Street 12, Ufa, 450008, Russia
[3]Kazan Federal University, Kremlyovskay St 18 Kazan, 450008, Russia
[4]Lomonosov Moscow State University, GSP-1, Leninskiye Gory, Moscow, 119991, Russia
[5]Saint Petersburg State University, Universitetsky pr. 28, Saint Petersburg, 198504, Russia

Received: September 30, 2015

Abstract. The effect of high pressure torsion (HPT) on the microstructure of Cu-Fe 36 wt.% alloy has been studied. The initial Cu-Fe alloy has a dendritic structure, the length of dendrites is up to 100 μm. As a result of HPT (20 anvil revolutions at 400 °C) a nanostructural state is formed. The average size of the Cu and α-Fe grains is 60 and 35 nm correspondingly. The volume fraction of the Fe phase reduces from the initial 37% down to 15% after HPT. The concentration of iron dissolved in the copper lattice reaches 20%. The subsequent annealing at 700 °C for 1 hour results in some coarsening of α-Fe particles, as compared to the state after HPT. However, the typical dendritic structure of the cast alloy does not recover; it remains dispersed with the size of α-Fe particles less than 20 μm. As a result of HPT the alloy microhardness increased from 1800 to 4000 MPa. The subsequent annealing at *T* = 700 °C decreased the microhardness to 2700 MPa, but this value is 1.5 times higher than that in the initial as cast state.

1. INTRODUCTION

The efficient method of formation of nanostructured (NS) states in metals and alloys is the severe plastic deformation (SPD). SPD techniques are based on the microstructure refinement to ultrafine (100-1000 nm) or nanometer (less than 100 nm) ranges by applying ultra-high degrees of plastic strain to materials under high pressure [1-4]. Due to the small grain size and large extent of grain boundaries, the NS materials have enhanced the mechanical and functional properties, thus opening new opportunities for their advanced applications in engineering and medicine [1-4].

Currently, the high pressure torsion (HPT) is a well-known SPD techniques, which enables achieving the highest strain degrees (*e >3-4*) without failure of billets under quasi-hydrostatic pressure [1,2]. Previously, homogeneous ultrafine-grained (UFG) and nanostructured (NS) states were produced via HPT in different metal materials, for example in pure Al, Cu, Ni [6-8], Fe and steel [9-14], aluminum [15-21] and titanium alloys [22-26]. Moreover, the microstructure refinement during SPD in alloys is often accompanied by phase transformations, dissolution and precipitation of second phases, their disordering and even amorphization [27-32]. During HPT of metallic alloys, besides the formation of UFG and nanostructural states, the change of the phase composition, the increase of metastability, phase solution, amorphization etc. take place [1-5,35-38]. Therefore of great interest are the peculiarities of phase transformations in SPD alloys formed by the

Corresponding author: A. Lukyanov, e-mail: alexlukjanov@yandex.ru

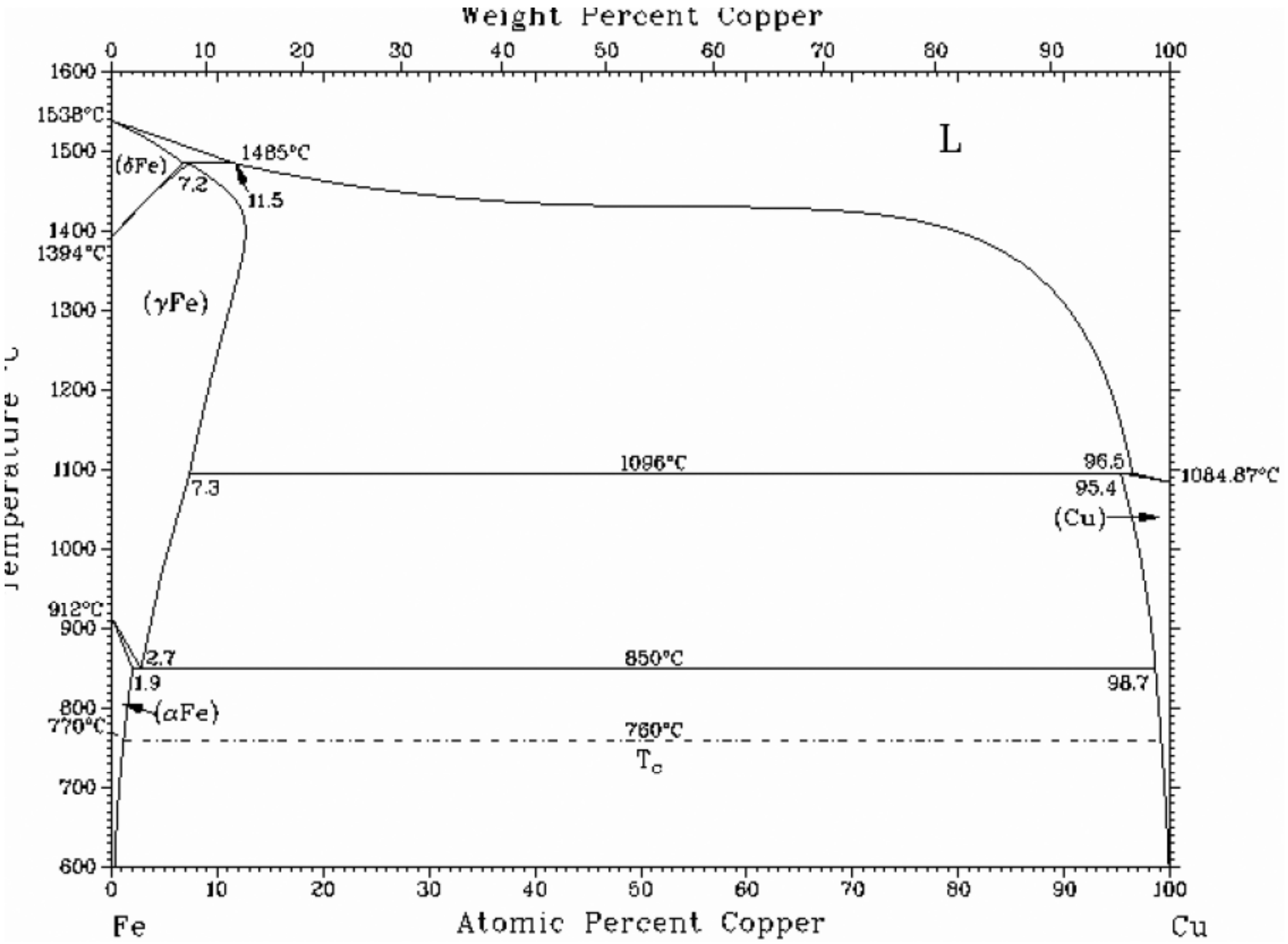

Fig. 1. Phase diagram of the iron-copper system.

components which are mutually insoluble in normal conditions, such as a Cu-Fe system alloys.

In [29,30] the effect of HPT on the mix of Cu and Fe powders with different ratios of components was studied at room temperature. It was shown that during SPD the formation of a nanocrystal (NC) structure together with the mutual dissolution of Cu and Fe occurs. So, in materials with high content of Cu (Cu-30% Fe) a solid solution of iron in copper is formed, in this case the fraction of Fe dissolved in Cu is up to 20% Fe. However, the studies of the impact of SPD on cast Cu-Fe alloys and of the subsequent annealing on the obtained samples are quite limited.

The interest in Cu-Fe alloys is explained also by their possible application as low-consumable anodes for aluminum production [33,34]. Copper and iron are not soluble in each other (Fig. 1). When these alloys crystallize, the coarse dendritic structure (fcc copper matrix and α-Fe dendrites) is formed. The possibility of corrosion penetration through the dendrites in the interior of the material may decrease its corrosion resistance at the electrolysis. The idea of applying SPD to Cu-Fe alloys is to transform the initial dendritic microstructure of the Cu-Fe alloy, assuming that this would enhance the corrosion resistance of the alloys and the effectiveness of their application as anodes. Besides, of great interest are the features of phase transformations during SPD of cast Cu-Fe alloy systems. Hence, the aim of this work was to study the changes in the microstructure and phase composition of the Cu-36% Fe alloy during the processes of HPT and subsequent annealing.

2. MATERIALS AND METHODS

In this work the samples of the cast alloy Cu-36%Fe (wt.) of 10 mm in diameter and 1.5 mm in thickness were subjected to HPT on grooved anvils with the number of revolutions 10 and 20 at 400 °C, at a pressure 6 GPa [1,2]. The shear strain at the edge of the sample was $\gamma \sim 450$ and 960, respectively.

Heat treatment of the samples after HPT was performed in a vacuum furnace at 700 °C for 1 hour (this temperature is a possible temperature for the operation of electrolytic cells and anodes in the aluminum production). The sample surface was polished and then etched in the acid mixture (50% of HNO_3 and 50% of HCl) for structural studies. The structure was investigated by the scanning electron microscope (SEM) JSM-6490LV Jeol and by

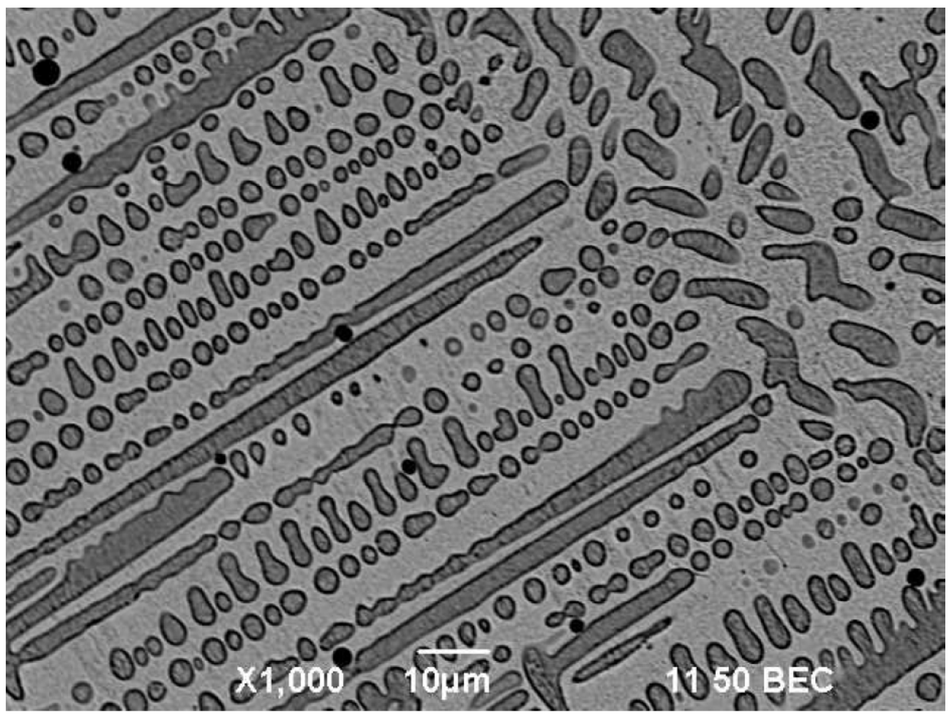

Fig. 2. SEM images of the cast Cu-Fe structure, magnification × 1000.

the transmission electron microscope (TEM) using a JEOL 2100 microscope operating at 200 kV. For TEM observations, samples were cut out at 3 mm from the disc, mechanically ground down to 150 μm and thinned by ion milling using a Jeol Ion Slicer at 5 keV.

The average sizes of structural elements and the phase fraction were estimated by 60-200 measurements.

The X-ray diffraction studies were performed on the diffractometer Rigaku Ultima IV with the use of Cu K_α–radiation ($\lambda_{K\alpha 1}$ = 1.540600 Å). The X-ray patterns were taken with the scanning pitch of 0.02° and the exposure time of 3 seconds in each point. The estimation of the structural parameters was performed by the Rietveld method using the software package PDWin. The microhardness H_v was determined on the Buehler «Micromet 5101» instrument.

3. RESULTS AND DISCUSSION

The microstructure of the cast Cu-Fe alloy is heterogeneous: it is represented by the Cu matrix and Fe columnar crystals with a distinct dendritic relief distributed in it (Fig. 2). Such parameters as the average length and width of major α-Fe dendrites, the average length and width of dendrite “branches”, the average sizes of α-Fe equiaxed grains were measured to describe the dendritic structure of the original cast alloy. The length of the major dendrite axes exceeded 100 μm and the width was about 10 μm. The major axes of the dendrites branch off up to 30 μm in length, 7-10 μm in width. The equiaxed inclusions of 5-10 μm other than the basic Fe dendrites of “skeletal” shape are observed.

HPT led to significant structural changes in the Cu-Fe alloy. As a result of HPT, the dendrites get

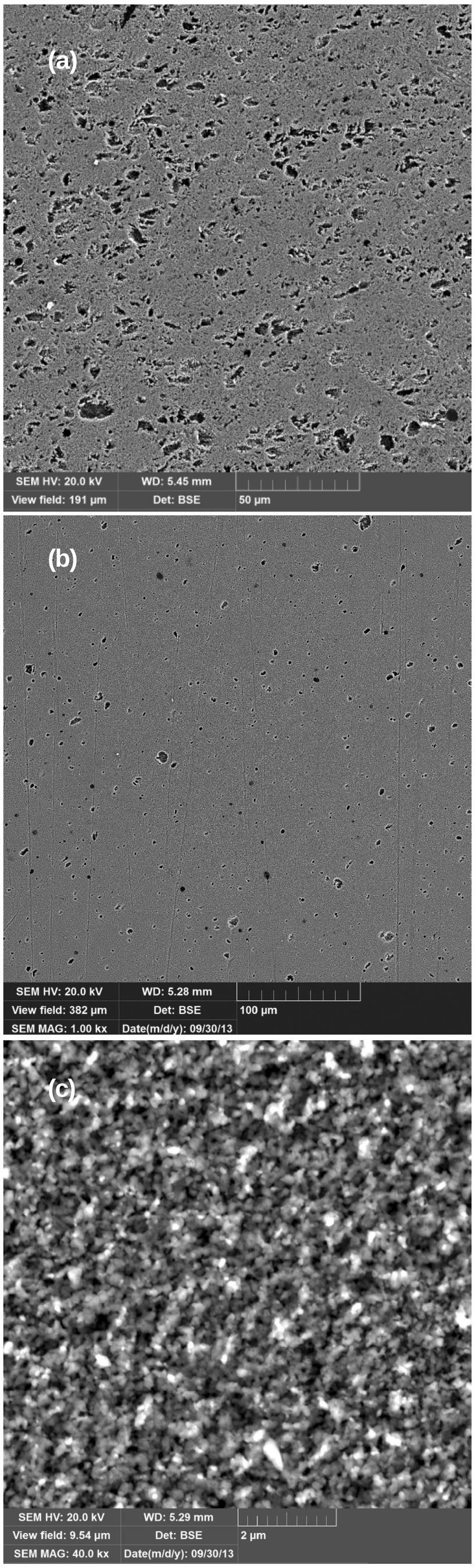

Fig. 3. SEM image of the Cu-Fe structure in the state after HPT at T = 400 °C, the edge of the sample: a) HPT n = 10 revolutions, magnification x 1000; b) HPT n = 20 revolutions, magnification × 1000; c) HPT n = 20 revolutions, magnification × 20000.

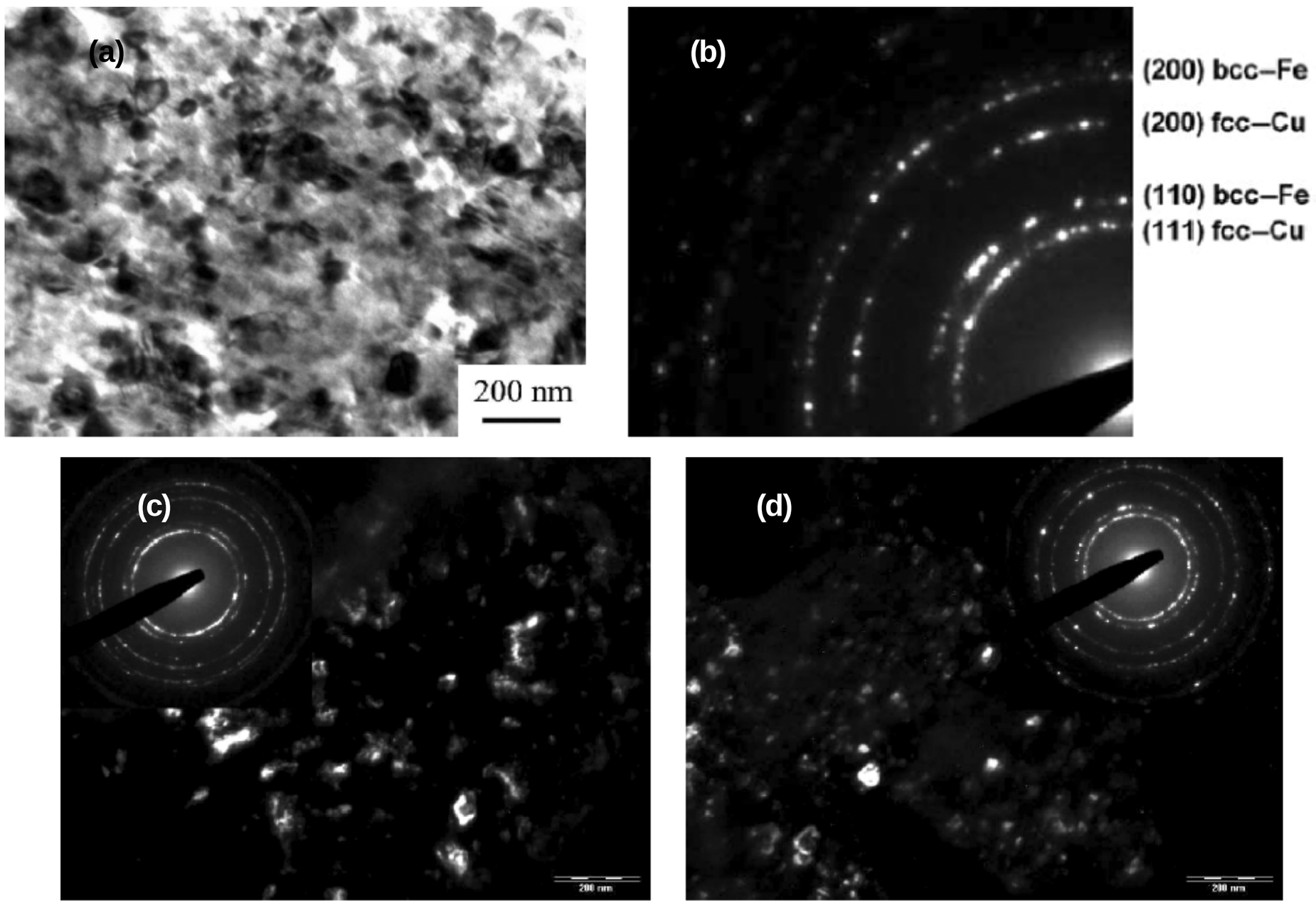

Fig. 4. Corresponding electron diffraction patterns and dark-field TEM images of the Cu–Fe composite after high pressure torsion (HPT) 10 revolutions where Cu (c) and α-Fe (d) phases are detected separately.

crushed and refined. According to the SEM image at the magnification of ×1000, after HPT 10 revolutions the maximum size of separate α-Fe inclusions in the copper matrix does not exceed 10 μm, and the α-Fe volume fraction significantly decreased as compared to the initial one (Fig. 3a). After HPT 20 revolutions the α-Fe volume fraction is further reduced, and the visible size of the α-Fe inclusions does not exceed 5 μm (Fig. 3b).

SEM study of the structure with high magnification (x 20000) shows that the copper and α-Fe structure after HPT (20 revolutions) is strongly refined, and the uniform nanocrystalline structure is formed (Fig. 3c). Precision structural investigations were performed using TEM–analysis studies at a samples after HPT. The microstructures of the composite after HPT processing in the bright and in the dark fields are shown in Fig. 4. After HPT 10 revolutions, nanoscaled grains with an equi-axed structure appear (Fig. 4a). The diffraction pattern (Fig. 4b) shows the rings characteristic for polycrystalline structures with a very small crystallite size. Both Cu and Fe phases are detected within the microstructure (Fig. 4a). The average grain size of Cu and Fe phases was detected by the dark field separately (Figs. 4c and 4d). The grain size of Cu was determined by the dark field image of the *(200)* Cu reflex, the grain size of Fe was determined by the dark field image of the *(200)* α-Fe reflex. The average grain size of the Cu - and α-Fe phase determined by the dark field is 60 and 35 nm correspondingly (Figs. 4c and 4d).

The annealing of the sample subjected to HPT at 700 °C for 1 hour results in some growth of α-Fe inclusions to 3-10 μm, although there are larger α-Fe precipitations reaching 20 μm in the structure (Fig. 5a). But the dendritic structure, typical for the cast state after HPT and annealing, does not recover, it remains dispersed, and α-Fe inclusions have an equiaxed shape (Fig. 5a). TEM-image of the Cu-Fe alloy structure after HPT at *T*=400 °C and subsequent annealing at 700 °C for 1 hour show that after the annealing the grain size is about 500 nm (Figs. 5b and 5c). Note that for pure copper after the HPT and the annealing at 500 °C the grain size reaches 2-3 μm [38]. Thus, the Cu-Fe alloy nanostructure after HPT reveals a very high thermal stability, explained by a disintegration of the solid solution formed by HPT and a mutual inhibition of grain growth on iron and copper particles.

X-ray diffraction analysis shows that HPT results in an approximately 2-fold increase of elastic microdistortions of the crystal lattice in the copper phase compared with those in the initial state (Table 1). The volume fraction of the Fe phase reduces from the initial 37% down to 15% after HPT (Table

Table 1. Results of the X-Ray diffraction study of the CuFe alloy.

State	$<\varepsilon 2>$, $\times 10^{-4}$	Cu lattice parameter, Å	Fe lattice parameter, Å	Fe volume fraction, %
Cast alloy	6	3.6168(2)	2.8716(2)	37
HPT T = 400 °C n = 20 revolutions	11	3.6293(4)	2.8706(4)	15
HPT T = 400 °C n = 20 + annealing T = 700 °C 1 h	8.5	3.6192(4)	2.8706(3)	25

Table 2. Results of the microhardness test measurements of the CuFe alloy.

State of the CuFe alloy	Range of measurements	Microhardness, MPa
Cast alloy	1800	
CuFe HPT n = 10	R	2570
	1/2R	2300
	Center	1900
CuFe HPT n = 20	R	4000
	1/2R	3700
	Center	3200
HPT T = 400 °C n = 20 + annealing 700 °C 1 h	1/2R	2700

1). Hence it can be concluded that more than a half of the iron present in the alloy is dissolved in copper, and the concentration of the iron dissolved in the copper lattice reaches 20%. In [29] at HPT of the mixture of Fe and Cu powders the atom probe analysis method applied to the $Fe_{50}Cu_{50}$ alloy was used in order to evaluate the possible formation of supersaturated solid solutions in the two-phase structures. The Cu concentration in the Fe phase is up to 25 at.% and the Fe concentration in the Cu phase is up to 20 at.%. Under the equilibrium conditions, the mutual solubility of Fe and Cu is normally less than 0.1 at.% at room temperature. Therefore, these data confirm that the formation of Fe supersaturated solid solutions as well as Cu supersaturated solid solutions is simultaneously possible in the two-phase structure. Note that the pattern of phase transitions observed in the present study is similar to that observed in [29].

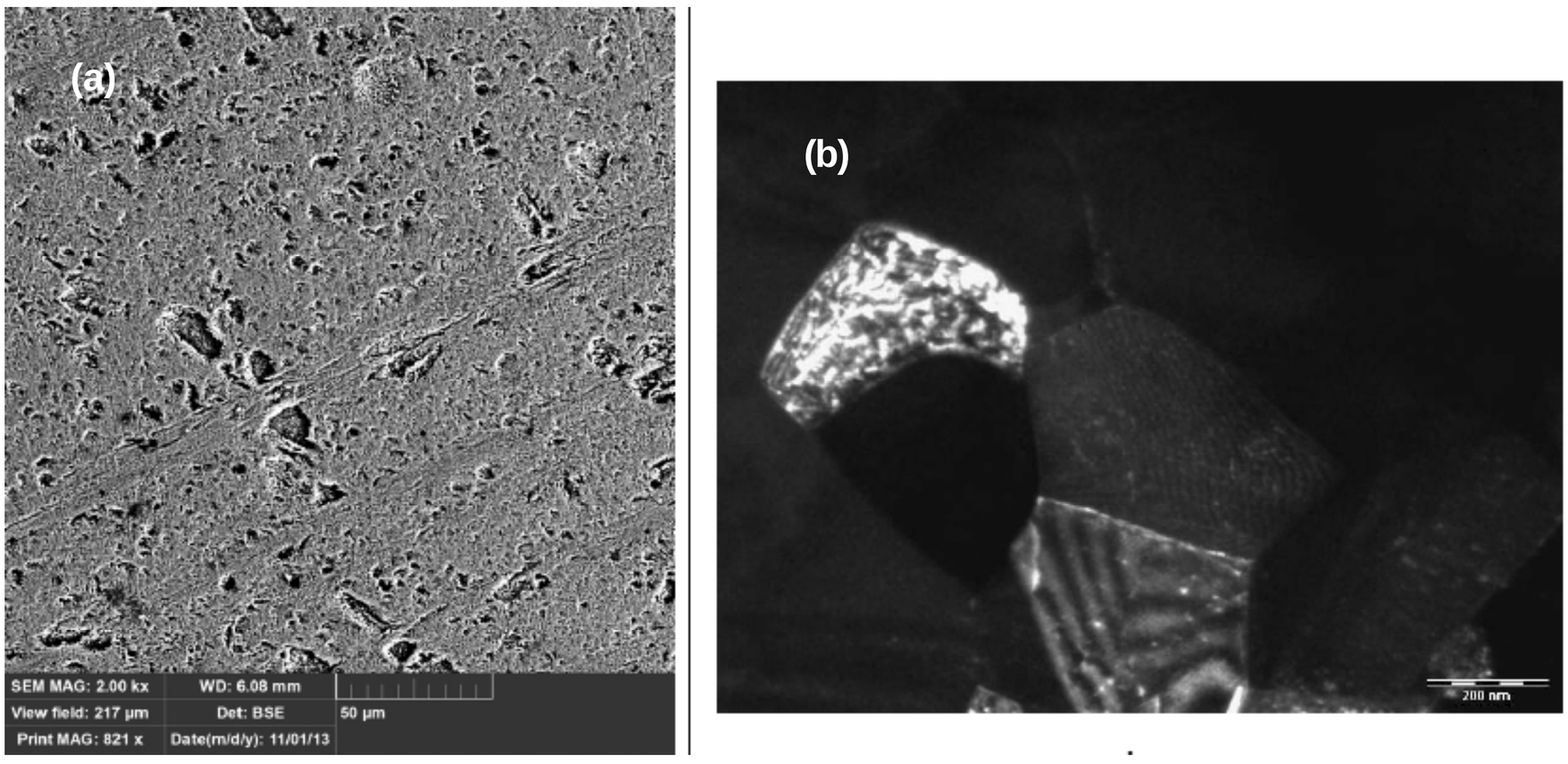

Fig. 5. The structure of Cu-Fe alloy after HPT at T = 400 °C and a subsequent annealing at the temperature 700 °C: a) SEM image with the magnification ×1000; b) TEM image (dark field) with the magnification ×20000.

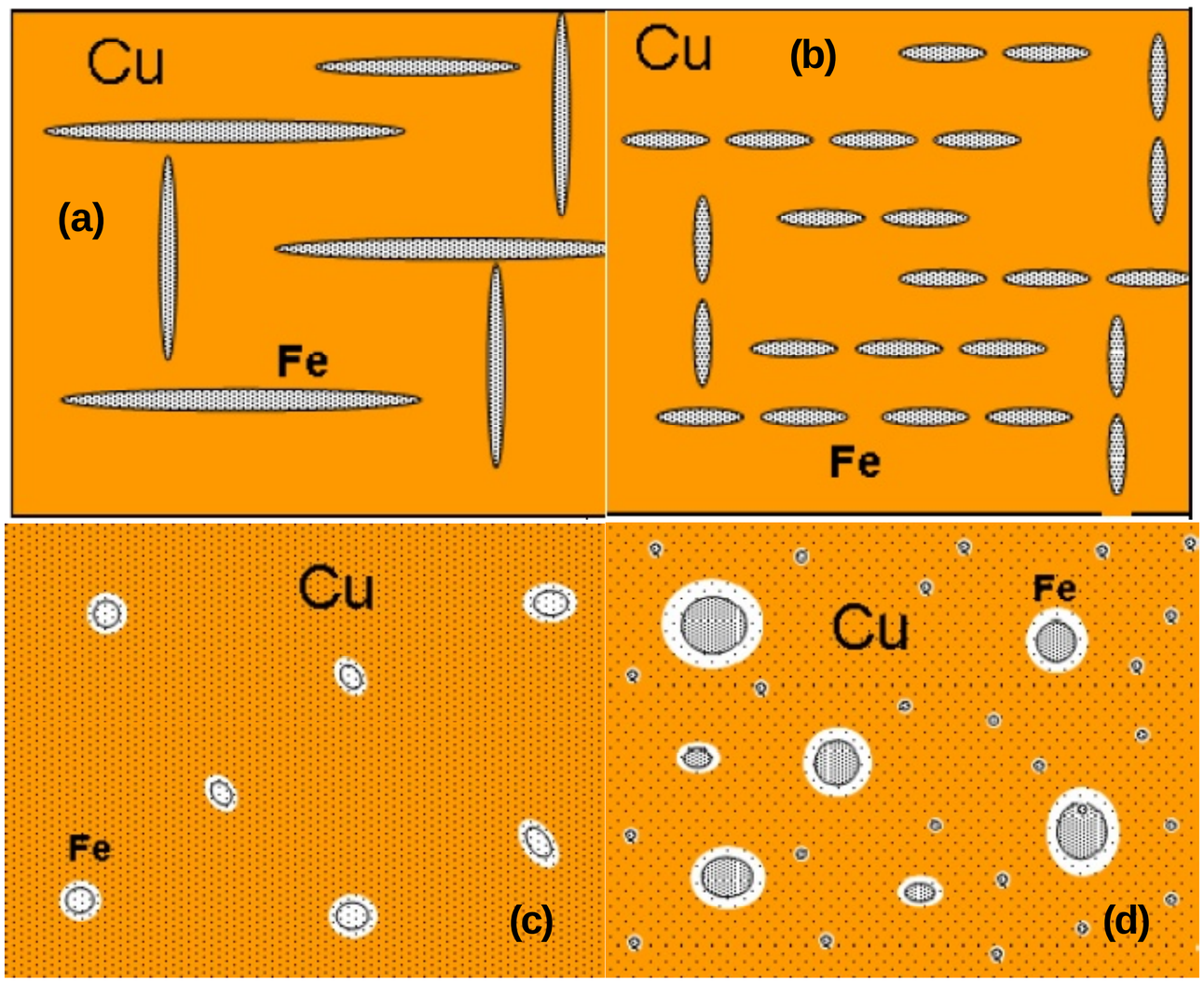

Fig. 6. Scheme of structural transformations in the alloy Cu-36%Fe at HPT and annealing: a) Fe dendrites in Cu matrix; b) refining of Fe dendrites at HPT; c) formation of a solid solution of Fe in Cu after HPT; d) HPT + annealing at 700 °C: nucleation and growth of Fe grains, and coarsening of Fe grains remaining after deformation.

After the annealing at 700 °C the crystal lattice microdistortions are reduced, and the Fe content is restored to a value close to the initial one. This is due to the decay of the supersaturated solid solution during the annealing, the coagulation and growth of Fe grains.

In the present study we have also investigated the effect of SPD and annealing of the CuFe alloy on its microhardness (H_v). It is known that HPT is inhomogeneous along the radius of the disk samples. The deformation rate is maximal at the edge of the sample (the “R” area) and minimal at the center [1-5]. In this regard, we measured the microhardness of CuFe samples after n = 10 and n = 20 revolutions of HPT in different regions of the sample disc: at the edge of the sample (the “R” area), at half-radius (1/2R) and in the center of the disk (Table 2). Microhardness measurements showed that the value H_v at the edge of the sample after HPT 10 revolutions increases to 2500 MPa, and after HPT 20 revolutions increases to 4000 MPa from the initial value of 1800 MPa. The H_v value noticeably grows with the increase of the number of HPT revolutions from 10 to 20. After HPT 10 revolutions and after HPT 20 revolutions the value H_v in the center of the disk sample is noticeably lower than at its edge. It follows that even at 20 revolutions of HPT the structure of the CuFe alloy sample remains radially inhomogeneous and the “strain saturation” does not occur. Note that, for example, in the case of pure copper even at n=5 revolutions of HPT the microhardness and the structure become nearly uniform over the area of the sample disk, and at further increase in the degree of HPT deformation (n>5) no additional structure refinement neither the increase in H_v is observed [2]. This is due to the fact that in most pure metals the processes of the refinement and the relaxation of the structure under HPT deformation become equilibrium at n = 5 revolutions or more [39]. At the same time, in CuFe alloys even at 20 HPT revolutions the equilibrium of the processes of the structure refinement and relaxation is not reached because the solid solution being formed and the copper and iron grains being intercalated inhibit the process of the dynamic recrystallization and relaxation.

Subsequent annealing at 700 °C (1 hour) of the CuFe sample, preliminarily subject to HPT 20 revolutions, reduces H_v from 4000 to 2700 MPa. However, this value is 1.5 times higher than H_v in the initial as-cast condition (Table 2). A high value H_v of the sample after the annealing also indicates a high thermal stability of the formed two phase structure.

The structural transformations occurring in the alloy after HPT and the annealing can be illustrated by the following scheme (Fig. 6).

As a result of HPT at the first stage the dendrites of Fe get crushed and refined. During the HPT the grain size is refined down to nanocrystalline, the area of intergranular and interphase boundaries

increase, a nonequilibrium state of grain boundaries is formed and the dislocation density within the grains increase. It accelerates the diffusion processes at HPT. A part of Fe atoms transfers to the solid solution of copper. However, fine nanocrystalline homogeneously distributed Fe particles with the fraction under 15% remain in the Cu matrix.

After annealing at 700 °C, a decay of the Fe–Cu solid solution formed after HPT takes place, resulting first in the nucleation and growth of Fe grains, and second, in the growth of Fe grains remained after the deformation.

Thus, HPT and subsequent annealing at a relatively high temperature allowed not only to significantly refine the structure of the cast Cu-Fe alloy, increasing its hardness. We note that such treatment also significantly changes the corrosion behavior of the alloy, which we plan to study in our future work.

4. CONCLUSIONS

i. It is established that during HPT the initial dendritic structure of the α-Fe cast alloy gets refined. The size of α-Fe particles after HPT ranges from 0.2 to 5 μm. It is shown that the α-Fe phase refinement degree is proportional to the HPT strain degree.

ii. After HPT the average grain size of the Cu - and α-Fe is 60 and 35 nm correspondingly. A volume fraction of the Fe phase reduces from initial 37% down to 15% after HPT. The concentration of iron dissolved in the copper lattice reaches 20%.

iii. The annealing after HPT at 700 °C for one hour resulted in the growth of α-Fe particles. However, the initial dendritic structure does not recover and is represented mainly by fine precipitates of 3-10 μm uniformly distributed in the Cu matrix.

iv. As a result of HPT and structure refinement, the microhardness increases from 1800 to 4000 MPa. Subsequent annealing at 700 °C (1 hour) reduces H_v to 2700 MPa, but this value is higher than in the initial as-cast condition.

ACKNOWLEDGEMENTS

The authors gratefully acknowledge the financial support of the samples preparation provided by the Russian Science Foundation through project No.14-12-00138. D.V. Gunderov acknowledges gratefully funding through the Russian Government Program of Competitive Growth of Kazan Federal University. A. Lukyanov and V. Pushin acknowledge Russian Science Foundation for the support № 15-12-10014 of Electron microscopy studies.

REFERENCES

[1] R.Z.Valiev, R.K.Islamgaliev and I.V.Alexandrov // *Prog. Mat. Sci.* **45** (2000) 103.
[2] R.Z. Valiev, A.P. Zhilyaev and T.C. Langdon, *Bulk Nanostructured Materials: Fundamentals and Applications* (John Wiley & Sons Inc., 2014).
[3] R.Z. Valiev, Y. Estrin, Z. Horita, T.G. Langdon, M.J. Zehetbauer and Y.T. Zhu // *JOM* **58** (2006) 33.
[4] Ruslan Valiev // *Nature Materials* **3** (2004) 511.
[5] A. P. Zhilyaev and T. G. Langdon // *Prog. Mater. Sci*. **53** (2008) 893.
[6] R. Pippan, S. Scheriau, A. Taylor, M. Hafok, A. Hohenwarter and A. Bachmaier // *Annu. Rev. Mater. Res.* **40** (2010) 319.
[7] M. Hafok and R. Pippan // *Philos. Mag.* **88** (2008) 20.
[8] R. Pippan, F. Wetscher, M. Hafok, A. Vorhauer and I. Sabirov // *Adv. Eng. Mater.* **8** (2006) 1046.
[9] Y. Ivanisenko, W. Lojkowski, R. Z. Valiev and H. J. Fecht // *Acta Mater.* **51** (2003) 5555.
[10] Y. Ivanisenko, R. K. Wunderlich, R. Z. Valiev and H. J. Fecht // *Scr. Mater.* **49** (2003) 947.
[11] Yu. Ivanisenko, N.A. Krasilnikov, F. Banhart, D. Kolesnikov, R. Valiev, W. Lojkowski and H.-J. Fecht // *Ann. Chim. Sci. Mat.* **27** (2002) 45.
[12] Yu. Ivanisenko, A.V. Sergueeva, A. Minkow, R.Z. Valiev and H.-J. Fecht, In: *Nanomaterials by Severe Plastic Deformation*, ed. by M. J. Zehetbauer and R.Z. Valiev (Wiley-VCH, Weinheim, Germany, 2004), p.453.
[13] J. Ivanisenko, A. Minkow, R.Z. Valiev and H.-J. Fecht // *Materials Science Forum* **558-559** (2007) 891.
[14] J.-L. Ning, E. Courtois-Manara, L. Kurmanaeva, A.V. Ganeev, R.Z. Valiev and Y. Ivanisenko // *Mater. Sci. Eng. A* **581** (2013) 8.
[15] I. Sabirov, M.Yu. Murashkin and R.Z. Valiev // *Materials Science and Engineering: A* **560** (2013) 1.
[16] R. Valiev, N. A. Enikeev, M. Y. Murashkin, V. U. Kazykhanov and X. Sauvage // *Scr. Mater.* **63** (2010) 4.
[17] R. K. Islamgaliev, N. F. Yunusova, R. Z. Valiev, N. K. Tsenev, V. N. Perevezentsev and

T. G. Langdon // *Scripta Materialia* **49** (2003) 467.
[18] G. Nurislamova, X. Sauvage, M. Murashkin, R. Islamgaliev and R. Valiev // *Phil. Mag. Lett.* **88** (2008) 459.
[19] V.N. Perevezentsev, M.Yu. Shcherban, M.Yu. Murashkin and R.Z. Valiev // *Tech. Phys. Lett.* **33** (2007) 648.
[20] R.Z. Valiev, M.Yu. Murashkin, E.V. Bobruk and G.I. Raab // *Mater. Trans.* **50** (2009) 87.
[21] M. Liu, H.J. Roven, X. Liu, M. Murashkin, R.Z. Valiev, T. Ungar and L. Balogh // *J Mater Sci* **45** (2010) 4659.
[22] I.P. Semenova, L.R. Saitova, G.I. Raab, A.I. Korshunov, Y.T. Zhu, T.C. Lowe and R.Z. Valiev // *Mater. Sci. Forum* **503-504** (2006) 757.
[23] I.P. Semenova, G.Kh. Salimgareeva, V.V. Latysh and R.Z. Valiev // *Solid State Phenomena* **140** (2008) 167.
[24] I.P. Semenova, R.Z. Valiev, E.B. Yakushina, G.H. Salimgareeva and T.C. Lowe // *J. Mater. Sci.* (2016), in press.
[25] J.M. Molina-Aldareguia, M.T. Perez-Prado, R.Z. Valiev, I.P. Semenova and I. Sabirov // *Int J Mater Form* **3** (2010) 407, (doi: 10.1007/s12289-010-0793-1).
[26] D.V. Gunderov, A.V. Polyakov, I.P. Semenova, G.I. Raab, A.A. Churakova, E.I. Gimaltdinova, I. Sabirov, J. Segurado, V.D. Sitdikov, I.V. Alexandrov, N.A. Enikeev and R.Z. Valiev // *Mater Sci & Eng A* **562** (2013) 128.
[27] X. Sauvage and R. Pippan // *Mater. Sci. Eng. A* **410–411** (2005) 345.
[28] I. Sabirov and R. Pippan // *Scripta Mater.* **52** (2005) 1293.
[29] X. Quelennec, A. Menand, J. M. Le Breton, R. Pippan and X. Sauvage // *Philos. Mag.* **90** (2010) 1179.
[30] A. Bachmaier, M. Kerber, D. Setman and R. Pippan // *Acta Mater.* **60** (2012) 860.
[31] D.V. Gunderov, A.V. Lukyanov, E.A. Prokofiev, A.R. Kilmametov, V.G. Pushin and R.Z. Valiev // *Materials Science and Engineering A* **503** (2009) 75.
[32] R.Z. Valiev, D.V. Gunderov, A.V. Lukyanov and V.G. Pushin // *Journal of Materials Science* **47** (2012) 7848.
[33] E. Antipov, A. Borzenko, V. Denisov, A. Filatov, V. Ivanov, S. Kazakov, P. Mazin, V. Mazin, V. Shtanov, D. Simakov, G. Tsirlina, S. Vassiliev and Yu. Velikodny // *Light metals* (2006) 403.
[34] A. Filatov, E. Antipov, M. Borzenko, S. Vasiliev, V. Denisov, V. Ivanov, S. Kazakov, Z. Kuzminova, V. Laurinavichyute, V. Lunin, D. Simakov and V. Shtanov // *Physical chemistry of surfaces and protection of metals* **44** (2008) 664, In Russian.
[35] Yu. Ivanisenko, N.A. Krasilnikov, F. Banhart, D. Kolesnikov, R. Valiev, W. Lojkowski and H.-J. Fecht // *Ann. Chim. Sci. Mat.* **27** (2002) 45.
[36] Yu. Ivanisenko, R.K. Wunderlich, R.Z. Valiev and H.-J. Fecht // *Scripta Mater.* **49** (2003) 947.
[37] Yu. Ivanissenko, W. Lojkowski, R.Z. Valiev and H.-J. Fecht // *Acta Mat.* **51** (2003) 5555.
[38] Jakub Cizek, Ivan Prochazka, Radomír Kuzel, Miroslav Cieslar and Rinat K. Islamgaliev // *Journal of Metastable and Nanocrystalline* **17** (2003) 37.
[39] E.I. Teitel, L.S. Metlov, D.V. Gunderov and A.V. Korznikov // *Physics of Metals and Metallography* **113** (2012) 1162.